

## Supporting Information

### Blue Luminescent N,S-doped Carbon Dots Encapsulated in Red Emissive Eu-MOF to Form Dually Emissive Composite for Reversible Anti-counterfeit Ink

JinPing Gao, RuXin Yao, XiaoHui Chen, HuiHui Li, Chao Zhang, FuQiang Zhang, Xian-Ming Zhang ,\*

Key Laboratory of Magnetic Molecules and Magnetic Information Materials, Ministry of Education, School of Chemistry & Material Science, Shanxi Normal University, Linfen 041004, P. R. China.

Corresponding Author

\*E-mail: zhangxm@dns.sxnu.edu.cn.

### Content

**Table S1.** Selected bond lengths [ $\text{\AA}$ ] and angles [ $^\circ$ ] for Eu-MOF.

**Fig. S1** Coordination modes of 1,3-db.

**Fig. S2** (a) PL spectra of Eu-MOF and the photo of Eu-MOF in sunlight and 365 nm UV lamp. (b) The lifetime of Eu-MOF.

**Fig. S3** The PXRD of Eu-MOF in different pH solution.

**Fig. S4** TG-DSC curves of Eu-MOF.

**Fig. S5** (a) The fluorescence pattern of Eu-MOF in volume ratio of 1:1 HCl and  $\text{Et}_3\text{N}$  and (b) the corresponding photos of fluorescence quenching and recovery from a-f.

**Fig. S6** (a) The Quantum Yield (QY) of Eu-MOF (b) The QY of Eu-MOF in ratio 1:1 HCl (c) The sample in ratio 1:1  $\text{Et}_3\text{N}$ .

**Scheme S1** The synthesis method of N,S-CDs.

**Fig. S7** (a) The TEM image and Particle size distribution pattern of N,S-CDs.(b)The high resolution TEM image of N,S-CDs.

**Fig. S8** (a) UV and PL spectra of the N,S-CDs. (b) The photographs of N,S-CDs at sunlight and UV light (365 nm).

**Fig. S9** The FTIR pattern of N,S-CDs.

**Fig. S10** Effect of pH on the Fluorescence intensity of N,S-CDs

**Fig. S11** (a) FL spectra of N,S-CDs aqueous solution at various excitation wavelengths. (b) Corresponding normalized emission spectra of N,S-CDs. (c) The CIE coordinate of N,S-CDs at different excitation wavelengths.

**Fig. S12** (a) FL spectra of N,S-CDs aqueous solution at various concentration. (b) Corresponding normalized emission spectra of N,S-CDs. (c) The CIE coordinates of N,S-CDs at different concentration.

**Fig. S13** (a) The PXRD and (b) FTIR patterns and of N,S-CDs, Eu-MOF and N,S-CDs@Eu-MOF.

**Fig. S14** The TEM of *N,S*-CDs@Eu-MOF.

**Fig. S15** (a) The fluorescence photos and (b) the corresponding PL spectra of Eu-MOF in ethanol mixture *N,S*-CDs various content aqueous solution. (c) amplification of the red emission peaks in (b).

**Fig. S16** (a) The fluorescence photos and (b) the corresponding PL spectra of Eu-MOF in acetonitrile mixture various content *N,S*-CDs aqueous solution. (c) amplification of the red emission peaks in (b).

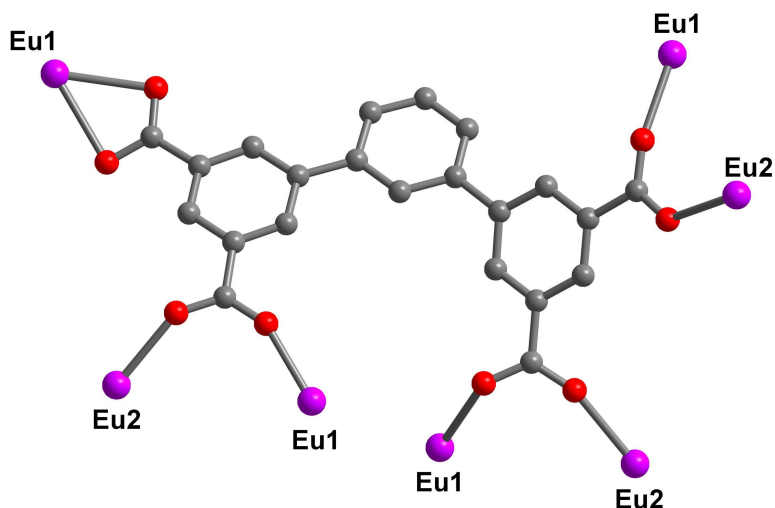
**Table S2** Selected ratiometric fluorescent sensors based on MOFs composite.

**Table S1.** Selected bond lengths [Å] and angles [°] for Eu-MOF

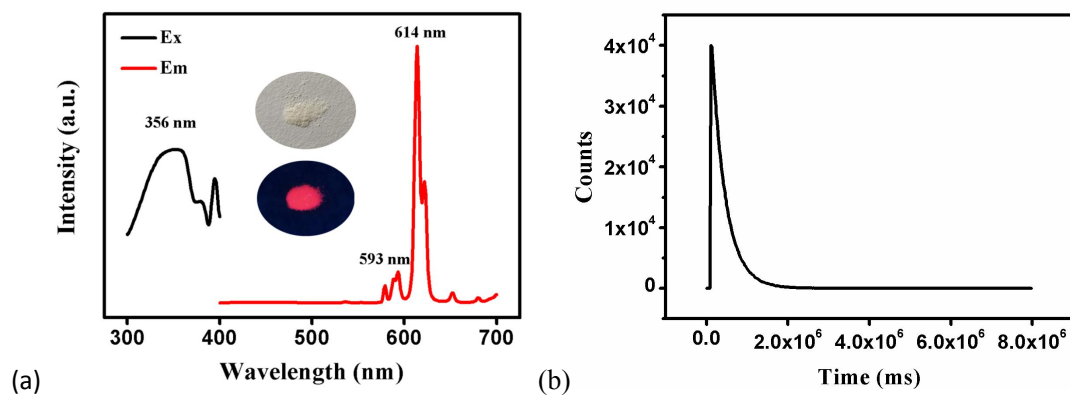
Eu-MOF			
Eu(1)-O(1a)	2.514(4)	Eu(2)-O(4e)	2.362(4)
Eu(1)-O(1)	2.515(4)	Eu(2)-O(4b)	2.362(4)
Eu(1)-O(2a)	2.433(5)	Eu(2)-O(5c)	2.346(4)
Eu(1)-O(3b)	2.295(4)	Eu(2)-O(5f)	2.346(4)
Eu(1)-O(6c)	2.360(4)	Eu(2)-O(8)	2.346(5)
Eu(1)-O(7d)	2.245(4)	Eu(2)-O(8d)	2.346(5)
Eu(1)-O(9)	2.459(6)	Eu(2)-O(11)	2.473(12)
Eu(1)-O(10)	2.419(5)		
O(1a)-Eu(1)-O(1)	67.45(15)	O(4e)-Eu(2)-O(4b)	139.7(2)
O(2a)-Eu(1)-O(1)	117.94(15)	O(4e)-Eu(2)-O(11)	72.3(3)
O(2a)-Eu(1)-O(1a)	52.48(14)	O(4b)-Eu(2)-O(11)	69.9(4)
O(2a)-Eu(1)-O(9)	85.2(3)	O(5f)-Eu(2)-O(4b)	99.61(16)
O(3b)-Eu(1)-O(1a)	128.13(15)	O(5f)-Eu(2)-O(4e)	82.48(17)
O(3b)-Eu(1)-O(1)	140.79(16)	O(5c)-Eu(2)-O(4e)	99.61(16)
O(3b)-Eu(1)-O(2a)	79.26(15)	O(5c)-Eu(2)-O(4b)	82.48(17)
O(3b)-Eu(1)-O(6c)	73.59(17)	O(5c)-Eu(2)-O(5f)	174.0(2)
O(3b)-Eu(1)-O(9)	73.7(2)	O(5f)-Eu(2)-O(11)	112.3(4)
O(3b)-Eu(1)-O(10)	143.85(19)	O(5c)-Eu(2)-O(11)	73.7(4)
O(6c)-Eu(1)-O(1b)	84.08(14)	O(8)-Eu(2)-O(4b)	140.36(15)
O(6c)-Eu(1)-O(1)	73.03(14)	O(8d)-Eu(2)-O(4e)	140.36(15)
O(6c)-Eu(1)-O(2a)	85.92(19)	O(8)-Eu(2)-O(4e)	77.10(17)
O(6c)-Eu(1)-O(9)	147.2(2)	O(8d)-Eu(2)-O(4b)	77.10(17)
O(6c)-Eu(1)-O(10)	142.51(17)	O(8d)-Eu(2)-O(5f)	75.42(16)
O(7d)-Eu(1)-O(1a)	148.18(15)	O(8)-Eu(2)-O(5c)	75.42(16)
O(7d)-Eu(1)-O(1)	83.85(15)	O(8)-Eu(2)-O(5f)	99.70(15)
O(7d)-Eu(1)-O(2a)	158.20(17)	O(8d)-Eu(2)-O(5c)	99.70(15)
O(7d)-Eu(1)-O(3b)	82.88(16)	O(8)-Eu(2)-O(8d)	74.8(3)

O(7d)-Eu(1)-O(6c)	100.97(16)	O(8)-Eu(2)-O(11)	131.4(4)
O(7d)-Eu(1)-O(9)	77.8(3)	O(8d)-Eu(2)-O(11)	146.8(4)
O(7d)-Eu(1)-O(10)	86.3(2)		
O(9)-Eu(1)-O(1)	138.1(2)		
O(9)-Eu(1)-O(1a)	114.4(2)		
O(10)-Eu(1)-O(1a)	72.03(17)		
O(10)-Eu(1)-O(1)	71.29(19)		
O(10)-Eu(1)-O(2a)	100.8(2)		
O(10)-Eu(1)-O(9)	70.3(2)		

**Symmetry code:** a)  $1/2-X, 1/2-Y, -Z$ ; b)  $-1/2+X, 1/2-Y, -1/2+Z$ ; c)  $1-X, +Y, 1/2-Z$ ; d)  $1/2-X, 1/2+Y, 1/2-Z$ ;  
e)  $1/2+X, 1/2+Y, +Z$ ; f)  $1/2+X, 1/2-Y, 1/2+Z$



**Fig. S1** Coordination modes of 1,3-db linker.



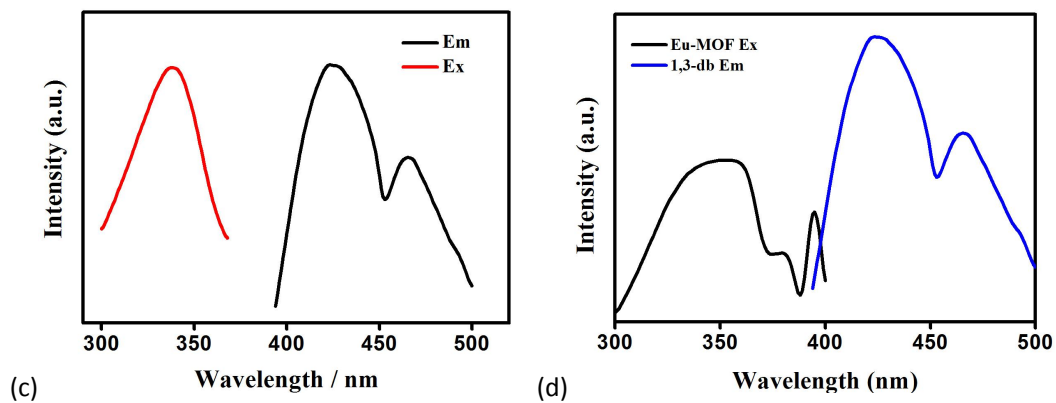


**Fig. S2** (a) PL spectra of Eu-MOF and the photo of Eu-MOF in sunlight and 365 nm UV lamp. (b) The lifetime of Eu-MOF. Excitation wavelength: 356 nm; Emission wavelength: 614 nm, 593 nm. (c) PL spectra of 1,3-db ligand. (d) Spectral overlap of the emission of 1,3-db and the excited of Eu-MOF

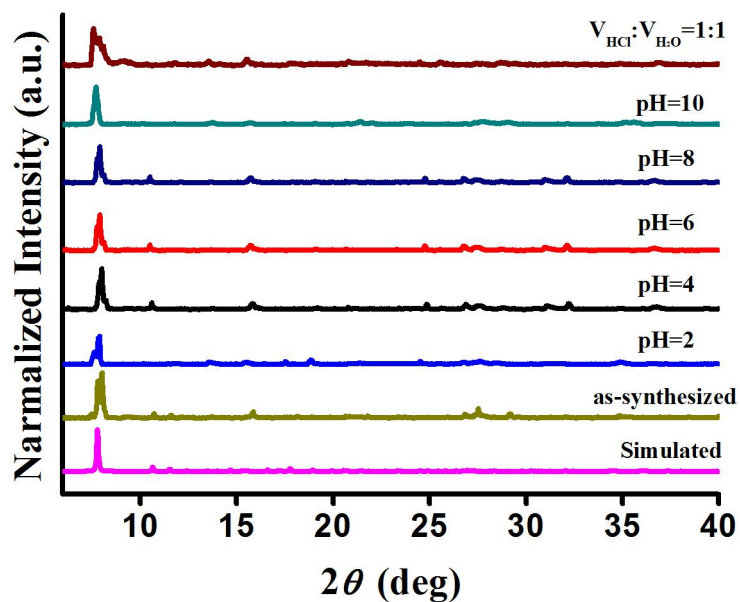


**Fig. S3** The PXRD of Eu-MOF in different pH solution.

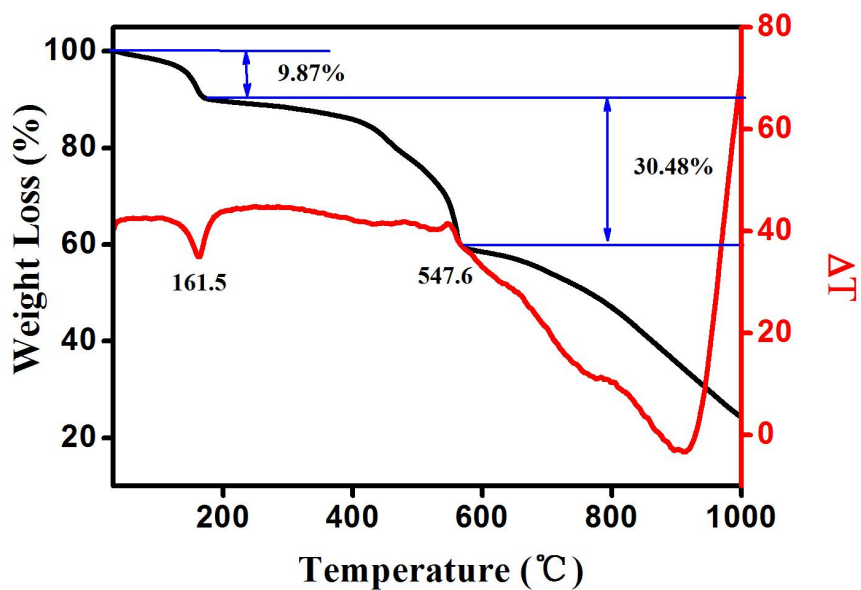


**Fig. S4** TG-DSC curves of Eu-MOF. Thermogravimetric analyses (TGA) indicate the free solvent molecules quickly loses weight in the temperature region of 30 ~ 160 °C and then shows obvious weight loss in the temperature region of 380 ~ 548 °C, the framework of Eu-MOF collapsed.

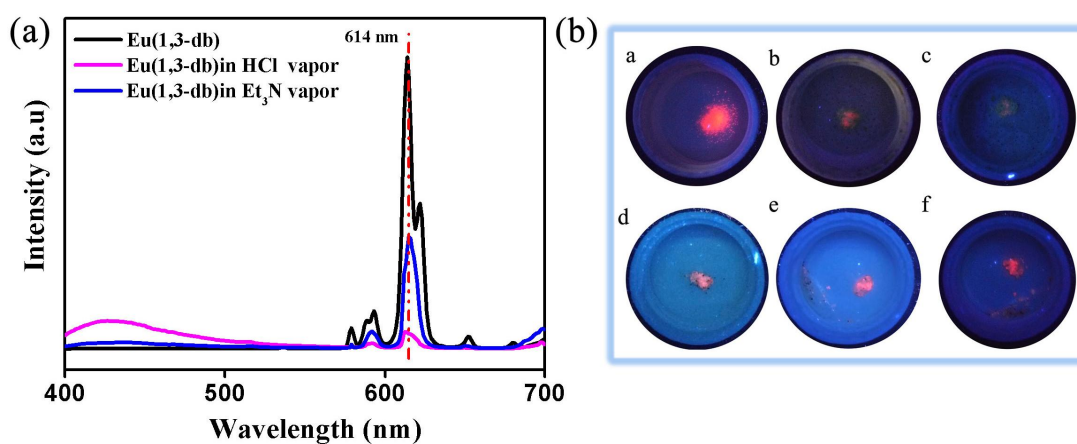


**Fig. S5** (a) The fluorescence pattern of Eu-MOF in volume ratio of 1:1 HCl and  $\text{Et}_3\text{N}$  and (b) the corresponding photos of fluorescence quenching and recovery from a-f.

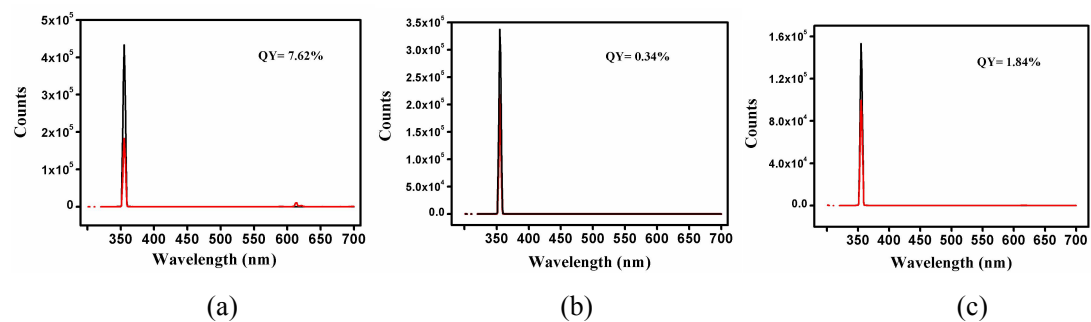
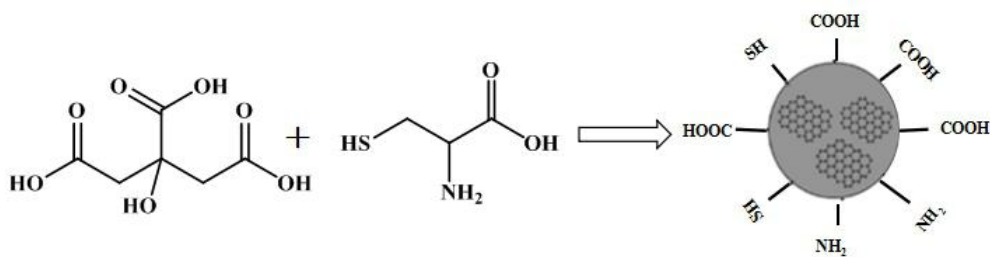


**Fig. S6** (a) The Quantum Yield (QY) of Eu-MOF (b) The QY of Eu-MOF in ratio 1:1 HCl (c) The sample in ratio 1:1 Et<sub>3</sub>N.



**Scheme S1** The synthesis method of *N,S*-CDs.

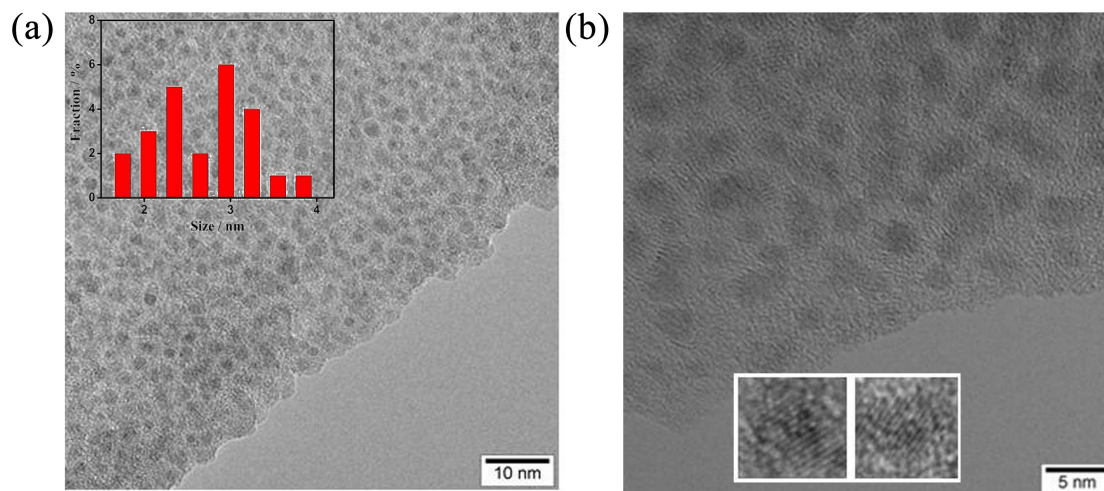


**Fig. S7** (a) The TEM image and Particle size distribution pattern of *N,S*-CDs. (b) The high resolution TEM image of *N,S*-CDs.

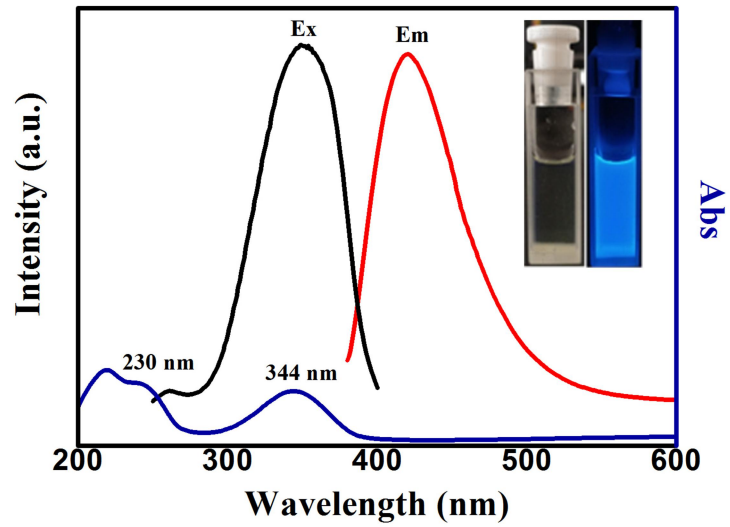


**Fig. S8** (a) UV and PL spectra of the *N,S*-CDs. (b) The photographs of *N,S*-CDs at sunlight and UV light (365 nm). Excitation wavelength: 360 nm; Emission wavelength: 426 nm.

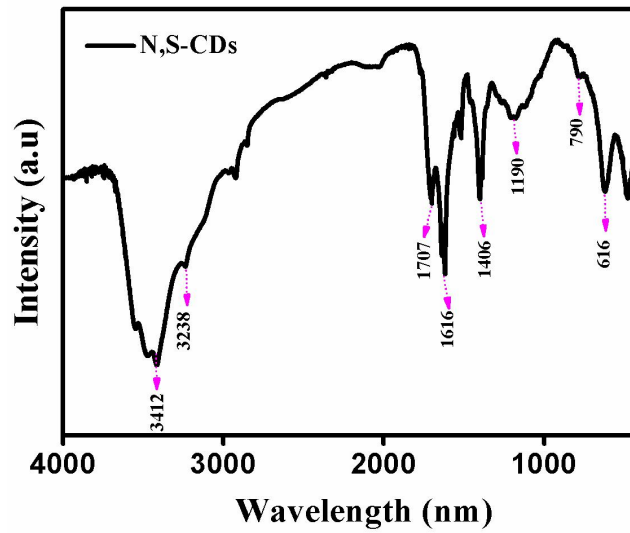


**Fig. S9** The FTIR pattern of *N,S*-CDs.

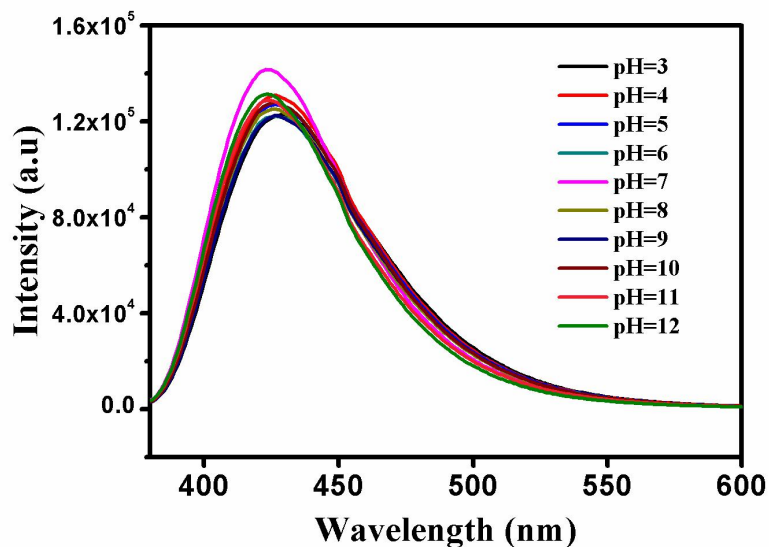


**Fig. S10** Effect of pH on the Fluorescence intensity of *N,S*-CDs. Excitation wavelength: 360 nm; Emission wavelength: 426 nm. There is no obvious change in the peak position of the emission peak of *N,S*-CDs in pH=3-12 aqueous, but the fluorescence intensity has a slight fluctuation, indicating that the material has strong acid-base stability.

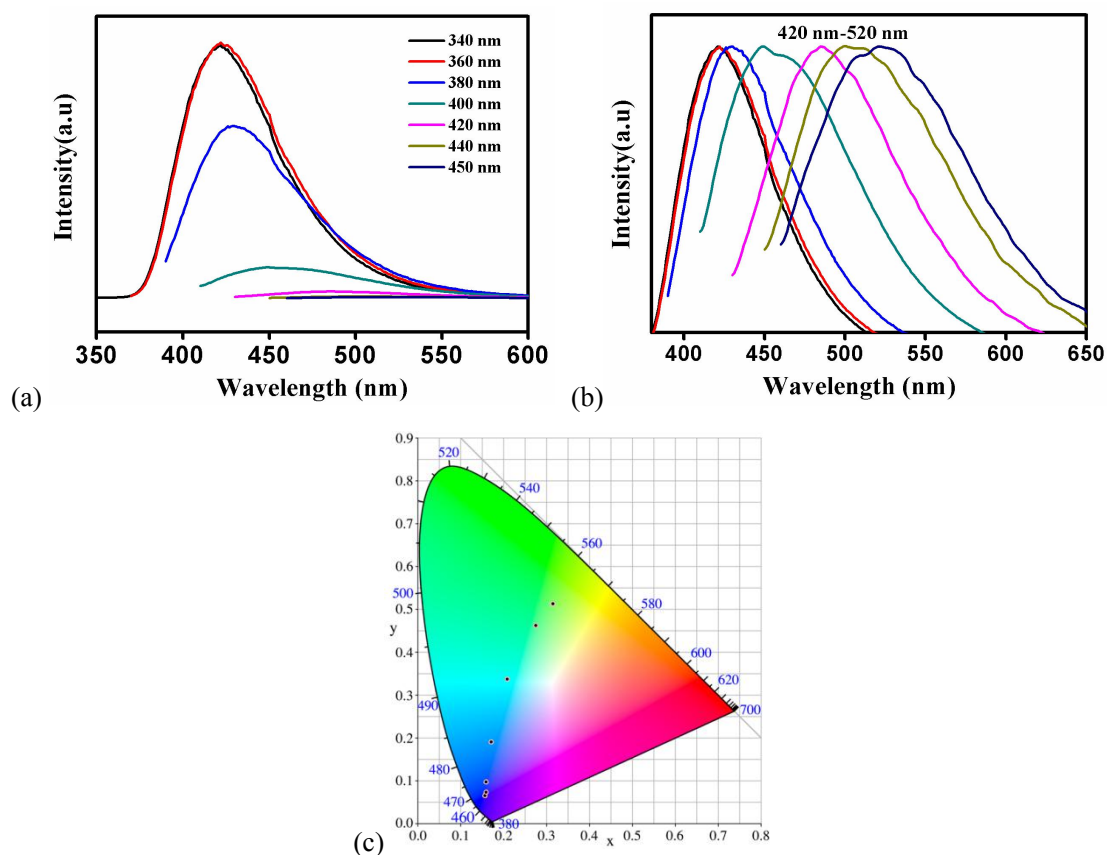


**Fig. S11** (a) FL spectra of *N,S*-CDs aqueous solution at various excitation wavelengths.(b) Corresponding normalized emission spectra of *N,S*-CDs.(c) The CIE coordinate of *N,S*-CDs at

different excitation wavelengths.

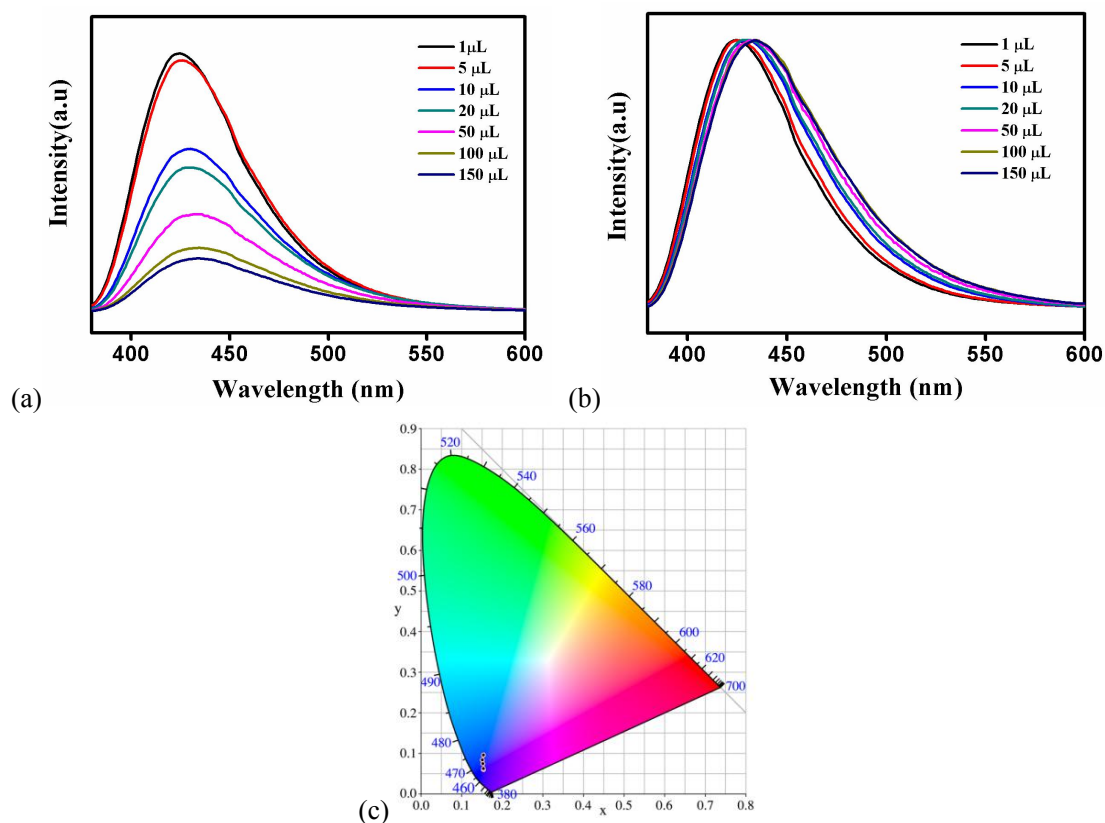


**Fig. S12** (a) FL spectra of *N,S*-CDs aqueous solution at various concentration. (b) Corresponding normalized emission spectra of *N,S*-CDs.(c) The CIE coordinates of *N,S*-CDs at different concentration.

The change of the fluorescence properties of *N,S*-CDs at different excitation wavelengths was tested (Fig. S11). As the excitation wavelength increases ( $Ex = 340\sim 450$  nm), the emission wavelength of the carbon dots is obvious. Moving toward the long wave ( $Em = 420\text{nm}\sim 520$  nm), and the fluorescence intensity tends to gradually weaken. In the normalized data, the emission peak at different wavelengths can also be seen to be red-shifted, corresponding to the color coordinates (Commission Internationale d' Eclairage (CIE 1931) chromaticity diagram) can be seen moving from the blue region to the green region, indicating that the emission spectrum of the carbon dots is red-shifted at different excitation wavelengths. Additionally, the FL intensity of *N,S*-CDs don't show significant change in a series of various concentrations (Fig. S12).

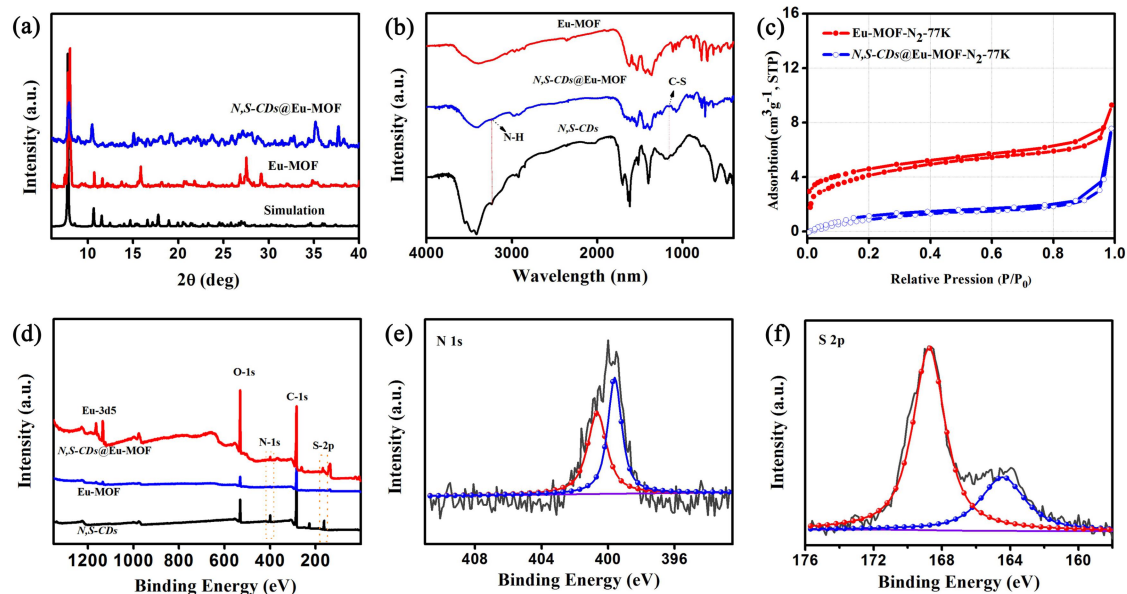


**Fig. S13** (a) The PXRD and (b) FTIR patterns and of *N,S*-CDs, Eu-MOF and *N,S*-CDs@Eu-MOF. (c) N<sub>2</sub> adsorption and desorption isotherms of Eu-MOF and *N,S*-CDs@Eu-MOF. (d) The XPS survey of *N,S*-CDs, Eu-MOF and *N,S*-CDs@Eu-MOF. (e) N 1s and (f) S 2p spectra of *N,S*-CDs@Eu-MOF.

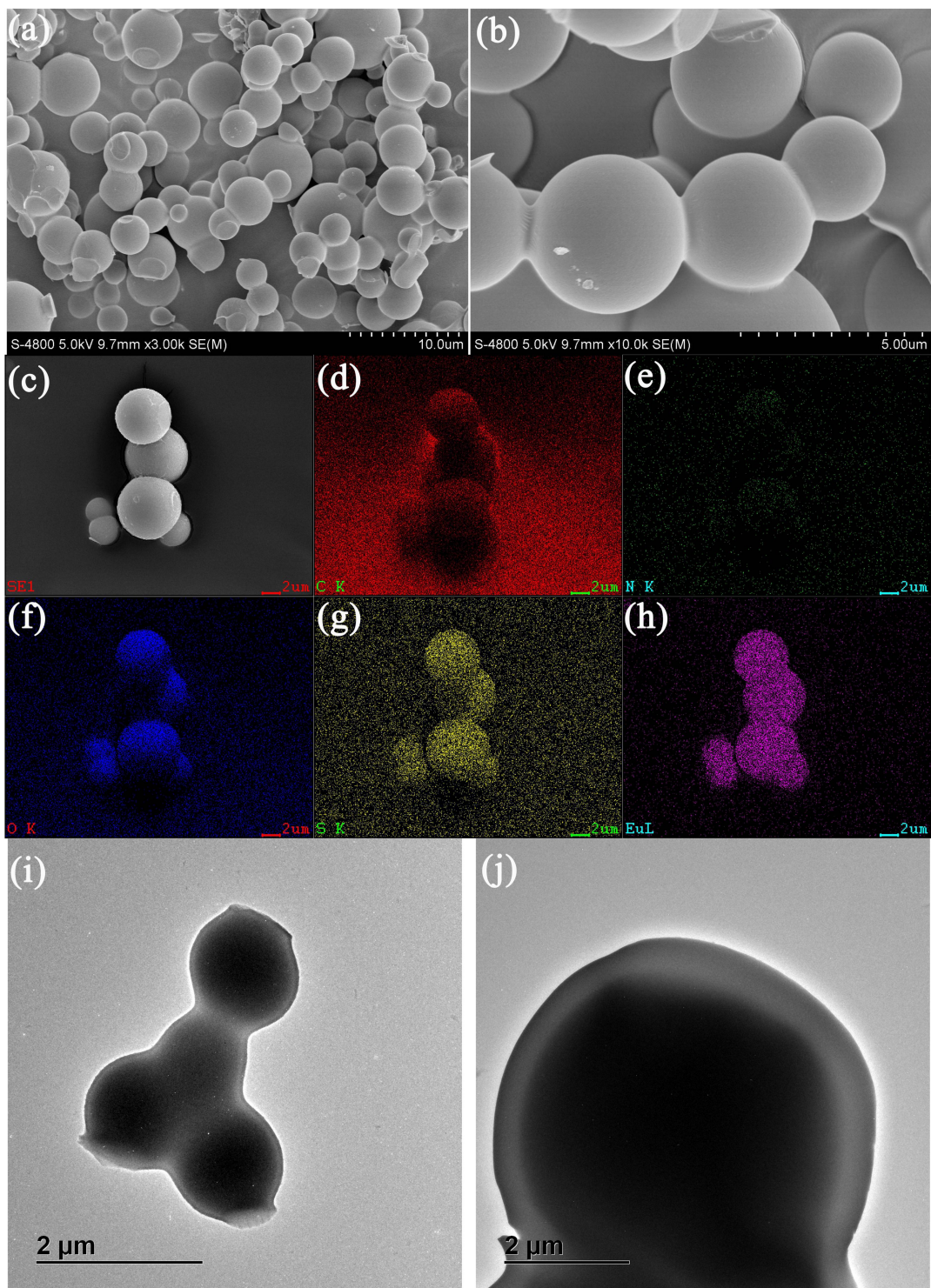


**Fig. S14** The SEM images (a-c) EDS-Mapping (d-h) the TEM images (i-j) of *N,S*-CDs@Eu-MOF.

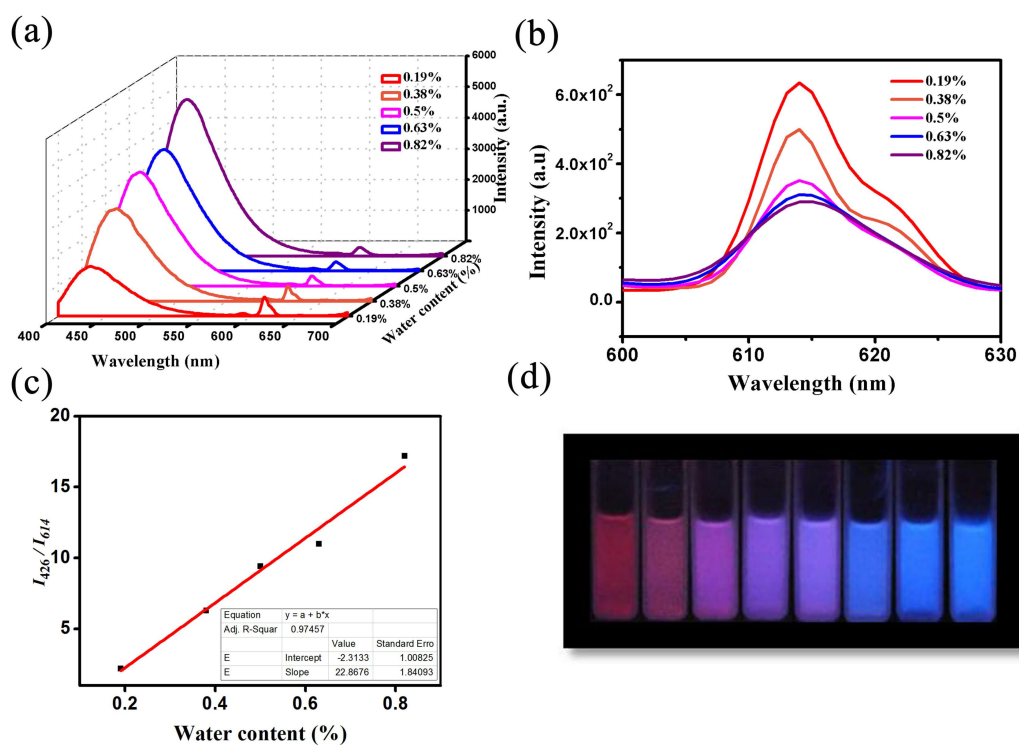


**Fig. S15** (a) The Fluorescence photos and (b) the corresponding PL spectra of Eu-MOF in ethanol mixture *N,S*-CDs various content aqueous solution. (c) amplification of the red emission peaks in (b).

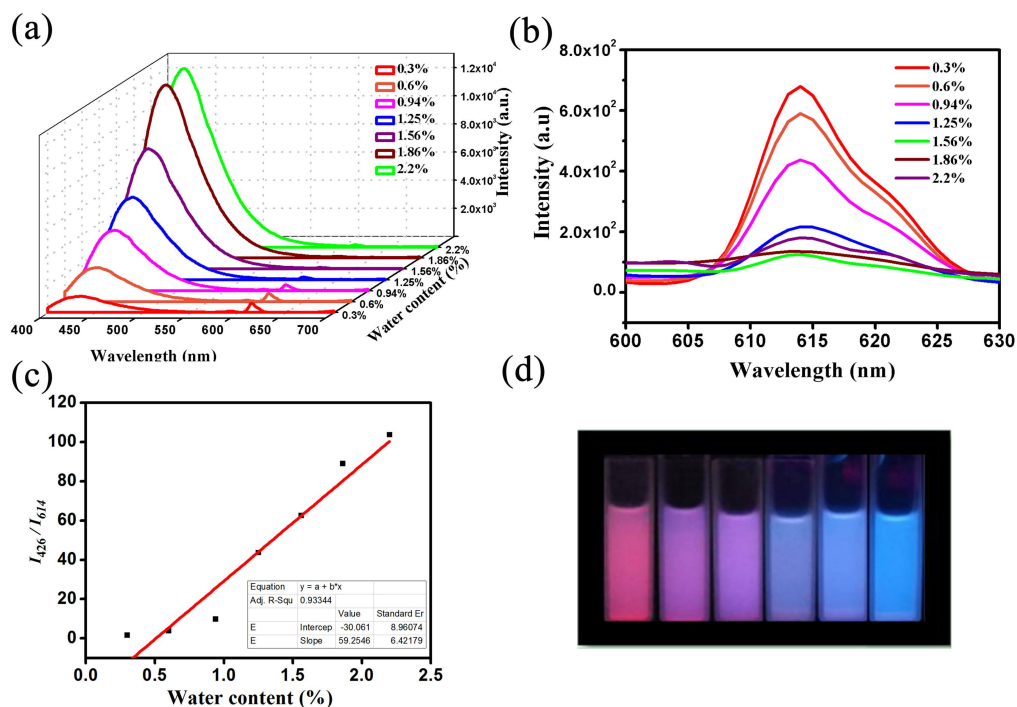


**Fig. S16** (a) The Fluorescence photos and (b) the corresponding PL spectra of Eu-MOF in acetonitrile mixture various content *N,S*-CDs aqueous solution. (c) amplification of the red emission peaks in (b).

**Table S2** Selected ratiometric fluorescent sensors based on MOFs composite.

compounds	Detection	examination range	Ref.
Ru@MIL-101(Al)-N H <sub>2</sub>	H <sub>2</sub> O	0–100%	Anal. Chem. 2017, 89, 13434
Tb <sup>3+</sup> @p-CDs/MOF	Humidity	33.0–85.1%	Dalton Trans. 2017, 46, 7098
Eu-MOF/N,S-CDs	H <sub>2</sub> O	0.05–4%	Anal. Chem. 2016, 88, 1748.
Eu-MOF@N,S-CDs composite	H <sub>2</sub> O in DMF	0.5%-2.5%	Our work
	H <sub>2</sub> O in C <sub>2</sub> H <sub>5</sub> OH	0.19 %-0.82 %	
	H <sub>2</sub> O in CH <sub>3</sub> CN	0.3%-2.2%	